The possibility of obtaining materials by plasma dynamic synthesis in the Ti-O system

A A Sivkov[1,2], Yu N Vympina[2], I A Rakhmatullin[2], A S Ivashutenko[2] and Yu L Shanenkova[1,2]
[1] College of Communication Engineering, Jilin University, Changchun, PR China
[2] School of Energy & Power Engineering, National Research Tomsk Polytechnic University, Tomsk, Russian Federation
E-mail: xyulyashax@mail.ru

Abstract. The possibility of obtaining a dispersed material by the method of plasma dynamic synthesis in the Ti-O system is shown. The plasma dynamic synthesis is based on the operation of a pulsed high-current coaxial magnetoplasma accelerator with titanium electrodes. The obtained product was investigated by X-ray diffraction method and transmission electron microscopy. The results showed the presence of two main titanium oxide (IV) crystalline modifications: anatase with tetragonal syngony and rutile also with tetragonal syngony. Moreover, the dominant modification is anatase in synthesized material.

1. Introduction

The problem of obtaining bulk ultrafine-grained materials and fine-dispersed powders of metals, alloys and compounds designed for various areas of technology has been discussed for a long time in the literature. Bulk ultrafine-grained materials can be obtained directly from bulk coarse-grained and amorphous materials or by powder metallurgy methods from fine-dispersed powders. In these days, interest in methods for obtaining superfine-grained bulk and dispersed materials has increased significantly, since it was found that a size decrease of structural elements (particles, crystallites, grains) below a certain threshold value can lead to a noticeable change in properties [1–5]. Such effects appear when the average size of crystalline grains does not exceed 100 nm.

The field of metal oxides is an important area in nanotechnology. Metal oxide nanostructures are applied in different fields of material science and engineering. For example, the main advantage of sensing and optical devices based on these materials arises from the high surface to volume ratio, favorable chemical stability, altered physical properties, confinement effects resulting from the nanoscale dimensions, and remarkable resistivity variation in gaseous environments. Additionally, the electrical conduction behavior of semiconducting metal oxide nanostructures and the proton conductivity of insulating metal oxide nanostructures commonly changes at different gaseous environments and by their dissociation of protons, making them promising materials for a wide range of eco-friendly and “green” applications [6].

From the discovery of superconductive oxides [7] and oxides with large magnetoresistance [8] the interest in these materials has increased even more, especially those of transition metal oxides [9]. Transition metal oxides are also commonly used as catalysts and in electronics, with applications varying from semiconductors, dielectrics, and conductive electrodes, which clearly demonstrates the importance and versatility of these materials [10].

The most common and widely used as sorbents and photocatalysts is titanium (IV) oxide due to a combination of properties such as low cost, chemical stability, catalytic activity. Moreover, in the nanoscale state, the particles of this material have an increased specific surface area, which positively affects its quantum efficiency [11–13]. There are many ways to synthesize nanoscale titanium dioxide, but none of the methods is universal in terms of the cost of precursors, time and simplicity of the process. For example, the well-known sol-gel method allows to obtain materials with both simple and complex chemical composition, in addition to regulate the particle size at any stage of the process [14–16]. However, the raw material has a high cost, the process of synthesizing the material is multistage. The solvothermal method also allows to control the particle size, the crystalline phases of the synthesized product [17, 18], but the rare material requires careful preparation. It is worth nothing that the whole process is strongly dependent on the reaction temperature, time, organic solvents.

The purpose of this work is plasma dynamic synthesis in the Ti-O system. It is assumed that it is possible to obtain titanium oxide (IV) with structural modification of anatase, which is more preferable for photocatalytic applications, in such a system. Unlike existing methods, plasma dynamic synthesis also allows to obtain nanoscale materials, while it is environmentally safe, one-step, fast (less than 10^{-3} seconds) and does not require additional preparation of precursors.

To achieve this goal, the following tasks have been set: 1) to obtain material by plasma dynamic synthesis in the Ti-O system; 2) to analyze the material by X-ray diffraction; 3) to analyze the product using transmission electron microscopy.

2. Experimental part

Plasma dynamic method is generally based on a system with a high-current (~ 100 kA) pulsed (~ 1 ms) coaxial magnetoplasma accelerator (CMPA) with metal titanium electrodes. A sketch-map of the coaxial magnetoplasma accelerator is shown in Figure 1.

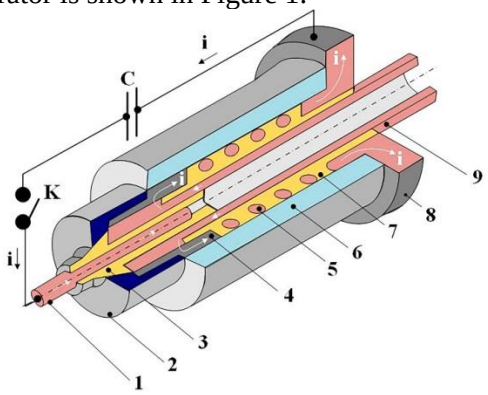

Figure 1. Sketch map, elements of coaxial magnetoplasma accelerator: 1) central electrode; 2) plug; 3) central electrode insulation; 4) contact cylinder; 5) solenoid; 6) case; 7) solenoid insulation; 8) contact flange; 9) electrode-barrel.

Titanium BT-1-O was used. Its phase composition was determined by X-ray fluorescence analysis. The results showed the presence, in addition to titanium, oxygen in the amount of 9%, chromium – about 1%. The presence of other elements (iron, silicon, copper, etc.) was less than 0.2%. The power supply of the CMPA is provided from a pulse capacitive energy storage device with a capacity of up to C_{ch} = 14.4 mF and a charging voltage up to U_{ch} = 2.5 kV. The energy stored by the capacitive energy storage device W_c, the amplitude of the discharge current of the power supply to the accelerator I_m, the developed power in the accelerating channel P_m, the energy W supplied to the accelerator can vary over wide ranges depending on U_{ch}. The initiation of the arc discharge between the central electrode and the electrode-barrel at the beginning of the accelerating channel was carried out by using of an electro-explosive carbon bridge deposited on the surface of the fiberglass insulator and electrically connecting the electrodes in the initial state.

After closing the power keys (K), a rising current begins to flow along the circuit. After some time, it reaches its critical value, which leads to the formation of a plasma structure inside the accelerating channel. As the jet moves, the electroerosion wear of the barrel occurs, the eroded material enters the plasma, thereby producing the base material, titanium. The expiration of a hypersonic plasma jet occurs in a sealed volume of a chamber-reactor filled with oxygen/argon gas (O_2/Ar). The synthesized product settles down to the wall of the chamber. After one hour, the chamber is opened and the product is collected. The experiment was carried out under the following conditions: C_{ch} = 14.4 mF, U_{ch} = 2.5 kV, accumulated energy W_c = 45 kJ, barrel length ℓ = 230 mm, barrel diameter d = 12 mm, O_2/Ar ratio – 1: 1, pressure in the chamber-reactor P = 1 atm., room temperature $t_0 \approx 20$ ° C.

To measure the rapidly changing voltage on the electrodes of the CMPA, ohmic voltage dividers are used. The discharge current characteristic is removed using a Rogowski transformer. Current and voltage signals are recorded on Tektronix TDS2012 oscilloscopes. Figure 2 shows the current and voltage waveforms recorded by digital oscilloscopes. It is seen that the peak values of voltage and current reach high values, up to 1.05 kV and 112 kA, respectively. These values are not constant, they depend on the capacitance and voltage of the capacitive energy storage device: the higher the charging voltage, the greater the discharge current and the voltage on the electrodes of the accelerator. By changing the capacity value, it is possible to regulate the time of the impulse process.

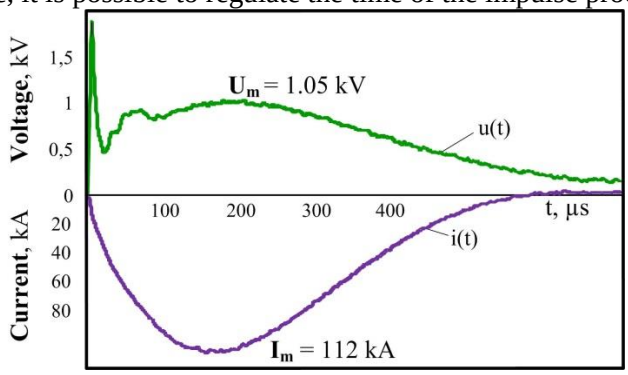

Figure 2. Wareforms of current i(t) and voltage u(t) on electrodes.

The power curves of the plasma discharge and the applied energy are shown in Figure 3. The maximum power value is 112 MW, and the sum of the energy supplied is 28.8 kJ.

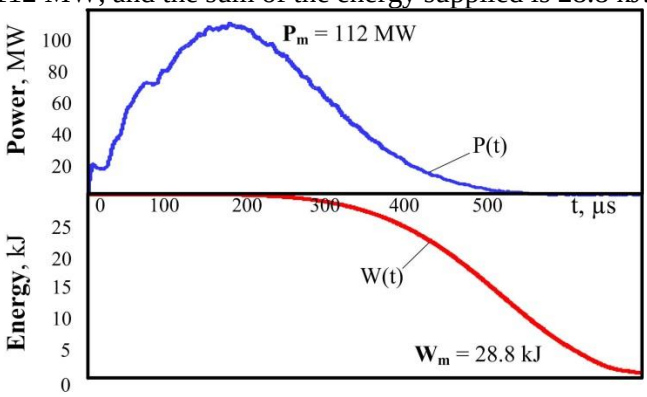

Figure 3. Power P(t) and energy W(t) curves.

3. Results and discussion

The product of plasma dynamic synthesis without additional preparation was investigated by X-ray diffractometry using Shimadzu XRD 7000S X-ray diffractometer (Cu-K_α). Figure 4 shows the X-ray diffraction pattern of the obtained product. The captured diffraction pattern is a set of coherent reflections of two titanium dioxide crystalline phase modifications: anatase aTiO_2 and rutile rTiO_2.

The structural models corresponding to the cards 21-1272 and 21-1276 are the closest to the found phases. Card numbers are taken from the PDF 4+ database.

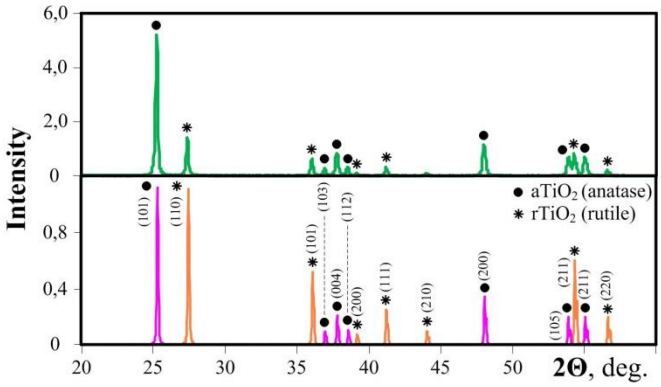

Figure 4. XRD patterns of product, synthesized by plasma dynamic method, and reference phases.

Processing and analysis of the XRD pattern was performed in PowderCell 2.4 software using the PDF 4+ database. The program made it possible to determine the quantitative ratios of the found phases, the size of the coherent scattering regions (CSR), and the levels of internal micro-distortions Δd/d. Table 1 shows the results of X-ray phase analysis.

Table 1. Results of X-ray diffraction analyze.

Phase, Space group	Content, (mass%)	CSR, nm	$\Delta d/d \cdot 10^{-3}$	Lattice parameters, Å Experimental /PDF, Å
$aTiO_2$ (anatase) 141/amd	61.7	97	1.3	a: 3.7844/3.7852 c: 9.5024/9.5139
$rTiO_2$ (rutile) P42/mnm	38.3	111	0.3	a: 4.5920/4.5933 c: 2.9578/2.9592

It is seen that the dominant modification is anatase. The difference in the lattice parameters of the identified phases from the standard values can be explained by the non-equilibrium and highly dynamic crystallization of the material. The consequence of this is quite high levels of internal micro-distortions. It can be concluded that materials are synthesized with defects. This fact can play a positive role in the processes of photocatalysis. According to numerous literatures, scientists are aware of the desire of scientists to obtain highly defective TiO_2 materials. Defects in the crystal lead to a decrease in the band gap and, as a consequence, a shift in the spectral absorption region of titanium dioxide from the ultraviolet region towards visible light [19].

To confirm some of the conclusions obtained from the results of X-ray phase analysis, the product of plasma dynamic synthesis was investigated by transmission electron microscopy. Figure 5 shows bright field TEM images of a cluster, a picture of selected area electron diffraction (SAED), and dark field TEM images of the same cluster. The specifics of sample preparation of highly dispersive materials for TEM exclude micron-sized particles from entering the sample.

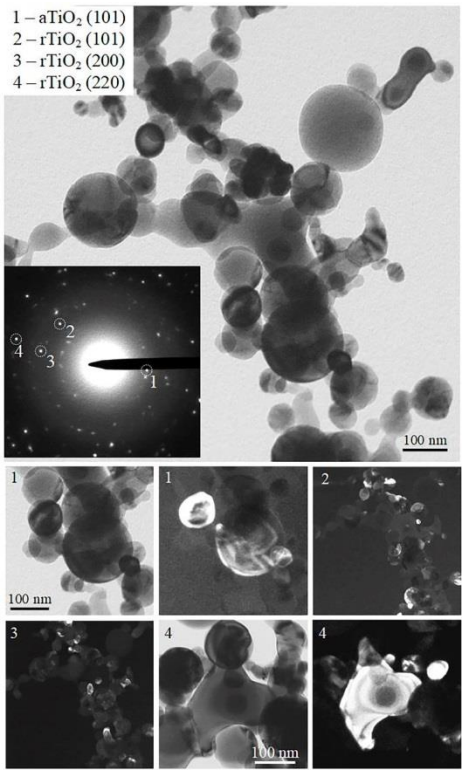

Figure 5. TEM images of synthesized product.

The material contains spherical particles with their size in the range of 27 ÷ 200 nm. At the same time there are shapeless objects whose length can exceed 100 nm. The SAED picture has a point-like appearance and contains reflections of two polymorphic phases of anatase and rutile.

It can be seen that some particles consist of several grains that belong to the structures of both anatase and rutile.

4. Conclusion

The paper presents the results showing the possibility of obtaining a nanostructured material by the plasma dynamic method in the Ti-O system. According to the results of X-ray diffraction analysis, 2 crystalline modifications of titanium dioxide were identified: anatase with tetragonal syngony and rutile with tetragonal syngony. The difference in the lattice parameters of the detected phases from the standard values can be explained by the non-equilibrium and highly dynamic crystallization of the material. The results of transmission electron microscopy showed that the minimum particle size is 27 nm. Moreover, some particles consist of several grains that belong to the structures of both anatase and rutile.

References

[1] Gleiter H 1992 *Nanostruct. Mater.* **1** 1–19 doi: 10.1016/0965-9773(92)90045-Y
[2] Siegel R W 1991 *Annu. Rev. Mater. Sci.* **21** 559–578 doi: 10.1146/annurev.ms.21.080191.003015
[3] Siegel R W 1993 *Nanostruct. Mater*. **3** 1–18 doi: 10.1016/0965-9773(93)90058-J
[4] Mayo M J 1997 *Nanostruct. Mater.* **9**(1–8) 717–726 doi: 10.1016/S0965-9773(97)00158-X
[5] Edelstein A S and Cammarata R C 1998 *Nanomaterials: Synthesis, Properties and Applications, Second Edition* (Florida: CRC Press) p 618
[6] Gangwar J, Gupta B K and Srivastava A K 2016 *Def. Sci. J.* **66** 323–340 doi: 10.14429/dsj.66.10206

[7] Cava R J 2000 *J. Am. Ceram. Soc.* **83** 5–28 doi: 10.1111/j.1151-2916.2000.tb01142.x
[8] Sun J Z and Gupta A 2003 *Annu. Rev. Mater. Sci.* **28** 45–78 doi: 10.1146/annurev.matsci.28.1.45
[9] Rao C N R, Muller A and Cheetham A K 2004 *The Chemistry of Nanomaterials: Synthesis, Properties and Applications* (Weinheim: WILEY-VCH Verlag GmbH & Co. KGaA, Weinheim) p 761
[10] Barquinha P, Martins R, Pereira L and Fortunato E 2012 *Transparent Oxide Electronics: from materials to devices* (Chichester: John Wiley & Sons) p 312
[11] Chung I 2012 *Nat.* **485**(7399) 486–489 doi: 10.1038/nature11067
[12] Huang H H 2004 *Scr. Mater.* **51**(11) 1017–1021 doi: 10.1016/j.scriptamat.2004.08.017
[13] Lilja M 2012 *Biotechnol. Let.* **34**(12) 2299–2305 doi: 10.1007/s10529-012-1040-2
[14] Trino L D 2018 *Coll. and Surf. A* **546** 168–178 doi: 10.1016/j.colsurfa.2018.03.019
[15] Attia S 2002 *J. Mater. Sci. Technol.* **18** 211–218
[16] Vorkapic D and Matsoukas T 2005 *J. Am. Ceram. Soc.* **81**(11) 2815–2820 doi: 10.1111/j.1151-2916.1998.tb02701.x
[17] Li G *et al* 2012 *J. Alloys Compd.* **532** 98–101 doi: 10.1016/j.jallcom.2012.03.050
[18] Liu J *et al* 2011 *ACS Appl. Mater. Interfaces* **3**(4) 1261–1268 doi: 10.1021/am2000642
[19] Amor C O *et al* 2019 *Phys. B: Condens. Matter* **560** 67–74 doi: 10.1016/j.physb.2019.02.017